Structure And Mechanical Behavior of Fully Substituted Acid Starch Esters

Adelina David, Grégory Stoclet, Nicolas Joly, Cédric Ribeiro, Nicolas Descamps, Denis Lourdin, Valérie Gaucher

RESEARCH ARTICLE

Macromolecular Chemistry and Physics
www.mcp-journal.de

Structure and Mechanical Behavior of Fully Substituted Acid Starch Esters

*Adelina David, Grégory Stoclet, Nicolas Joly, Cédric Ribeiro, Nicolas Descamps, Denis Lourdin, and Valérie Gaucher**

This study deals with the evolution of structural, thermal, and mechanical properties of a series of fully substituted fatty acid starch esters (FASEs) according to side chain length (from 2 (C2) up to 16 (C16) Carbons). FASEs with C2 to C12 side chains are fully amorphous with a glass transition temperature depending on chain length while in the case of FASE with C16 side chains, a part of side chains is able to crystallize. Thermomechanical behavior depends strongly on both the alkyl chain length and crystallinity of samples. In particular, for FASE-C16, the presence of crystals leads to a brittle behavior. During stretching, no macromolecular orientation is evidenced for short-chain FASEs (<C8), whereas, for long-chain starch ester from C8 to C16 length, an orientation of starch backbone in the drawing direction is observed.

1. Introduction

Among natural materials, starch appears as an attractive candidate for the substitution of petroleum-based polymers. Indeed, starch is abundant, cheap, renewable, and relatively easy to isolate in a highly pure form. This polysaccharide is composed of two different macromolecules: amylose, an essentially linear macromolecule, and amylopectin, a highly branched polymer. The ratio of amylose/amylopectin depends upon the botanic source. In the context of environmental concerns, starch has received a lot of attention in the last 20 years, as evidenced by the numerous reviews in the literature.[1–7] However, thermoplastic starch (TPS) films obtained by destructuring native starch granules exhibit some drawbacks, such as their high hydrophilicity due to their intrinsic high density of hydroxyl functions, its limited processability, and its poor mechanical properties, as compared to conventional synthetic polymers, particularly regarding its stretchability which limits its use to low-performance applications.[8]

Plasticization is commonly used to overcome the previously discussed limitations of starch. Besides, starch can be plasticized with external plasticizers, such as water,[9] polyols like glycerol,[10] glycols,[11] amides,[12] or ionic liquids,[13] notably. Even if this route leads to biodegradable starch which has found some applications for packaging and agricultural purposes, some shortcomings, such as plasticizer migration, induce an evolution of its properties with time and thus limit its applications.[14] To overcome some of these drawbacks and to achieve the desired product properties, the natural polymer can be modified by chemical routes for example by substituting some hydroxyl function with other chemical functional groups such as ether or ester groups,[15] or by grafting chains as a copolymer of poly (butyl acrylate-co-styrene).[16] Esterification of starch with organic acids is one way that allows obtaining starch ester with a high substitution degree (DS) even with long alkyl chains, leading to less hydrophilic products. Literature reports several studies dedicated to the synthesis of esterified starch with acid derivatives,[17–19] as well as to the evaluation of side chain length influence on the structure and thermomechanical behaviors of fully substituted fatty acid starch esters (FASEs).[20–22]

Structural characterizations and thermal analysis have shown that starch ester derivatives self-organize in a layered structure as for cellulose esters,[23] for which a model has been proposed.[20,24]

A. David
Institut Français des Matériaux Agro-Sourcés (IFMAS)
60 Avenue du Halley, Villeneuve-d'Ascq 59650, France
A. David, G. Stoclet, C. Ribeiro, V. Gaucher
Université Lille
CNRS
INRAE
Centrale Lille
UMR 8207 – UMET – Unité Matériaux et Transformations, Lille F-59000, France
E-mail: valerie.gaucher@univ-lille.fr
N. Joly
Univ. Artois
Unilasalle
ULR7519—Unité Transformations & Agro-Ressources
Béthune 62408, France
N. Descamps
Roquette Frères
Lestrem Cedex 62080, France
D. Lourdin
UR 1268 Biopolymeres Interactions Assemblage
INRA
Nantes F-44300, France

The ORCID identification number(s) for the author(s) of this article can be found under https://doi.org/10.1002/macp.202300177

DOI: 10.1002/macp.202300177

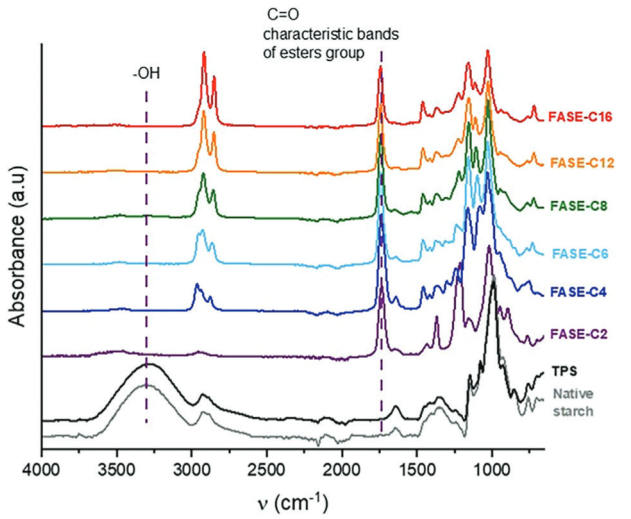

Figure 1. FTIR spectra of native waxy maize starch, TPS, and all fatty acid starch esters.

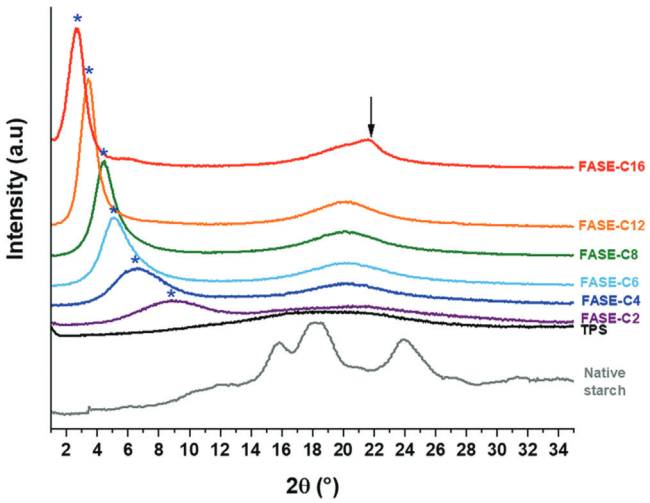

Figure 2. WAXS profiles of fatty acid starch triesters, thermoplastic, and native waxy maize starches.

Regarding the mechanical properties of these materials, the evolution of the yield stress seems to show no clear trend while a decrease in the drawability has been highlighted when the length of the fatty side chain is increased.[20,22]

The synthesis and thermal properties of starch grafted with alkyl chains having different lengths from C2 to C16 have already been described in the literature.[20–22] However, a review of the literature shows some discrepancies regarding the results obtained, probably due to the fact that the synthesis methods and starch origin differ according to the studies. The influence of the alkyl chain length on mechanical behavior remains poorly addressed in the literature. Particularly the mechanical behavior of butyrate (C4) and hexanoate (C6) starch esters is scarcely studied. Moreover, the literature review concerning the study of palmitate (C16) starch ester shows controversial results. For example, depending on the studies, the stretchability and the stress levels of starch palmitate strongly vary.[20–22] In addition to the few data available regarding their mechanical properties, their structural evolution upon stretching, has never been studied to the best of our knowledge.

In this context, we synthesized fully substituted FASEs, starting from waxy maize starch, with alkyl chain lengths ranging from C2 to C16. The goal of this study is to get an in-depth characterization of starch ester structure as a function of chain length and the structural evolution of materials with temperature. The macromolecular orientation during the uniaxial stretching test as a function of the alkyl chain length was also investigated in order to determine the respective roles of starch backbone and grafted chains on the mechanical behavior.

2. Results and Discussion

2.1. Chemical Characterization

FTIR spectra of native waxy maize starch, TPS, and all starch esters are depicted in **Figure 1**. While the spectra of native starch and TPS are similar, a complete disappearance of the characteristic band of hydroxyl group at 3300 cm^{-1} (OH stretching) is observed for all the starch esters, suggesting the complete substitution of OH groups by fatty acid chains. An increase in the intensity of the C—H alkyl bonds characteristic signals at 2800–2900 cm^{-1} (CH antisymmetric and symmetric stretching of CH_2 and CH_3), concomitant to the appearance of a new band around 1740 cm^{-1} attributed to the stretching of carbonyl ester groups, confirm the presence of fatty chains. The intensity differences regarding the alkyl bands at 2800–2900 cm^{-1} are due to the number of successive methylene groups present in the fatty acid chains: the intensity of this band increases with fatty chain length.

^{1}H NMR spectroscopy was used to quantify the degree of substitution (DS) of OH groups by fatty acid chains. The spectra are available in Supporting Information. The acylation of starch was confirmed by the integration of the characteristic signals of fatty acid protons from 0.89 to 2.34 ppm and of the starch backbone from 5.50 to 3 ppm (carbohydrate protons). The DS for each starch ester was estimated to be 2.8 ± 0.1.

2.2. Structural and Thermal Characterization as Function of the Alkyl Chains Length

2.2.1. Structural Characterization

Figure 2 depicts the wide angle X-ray scattering (WAXS) integrated intensity profiles of as-molded films including TPS and the native starch for comparative purposes. While the native waxy maize starch shows diffraction peaks characteristic of A-type crystallinity (diffraction peaks at $2\theta \approx 15°$ and 24° and the doublets at 17°–18°),[25,26] TPS film is fully amorphous as evidenced by the presence of an only broad halo around 20°. The FASE-C2 to FASE-C12 starch esters are also amorphous. In addition, regarding FASE-C16, a weak diffraction peak is observed around $2\theta \approx 22°$ (↓ Figure 2), superimposed to the amorphous halo. A comparison with the literature indicates that the position of this peak does not correspond to the one reported for the various starch crystalline structures.[27] Moreover, this peak has already been observed in other studies dealing with FASEs,[20] and fatty acid

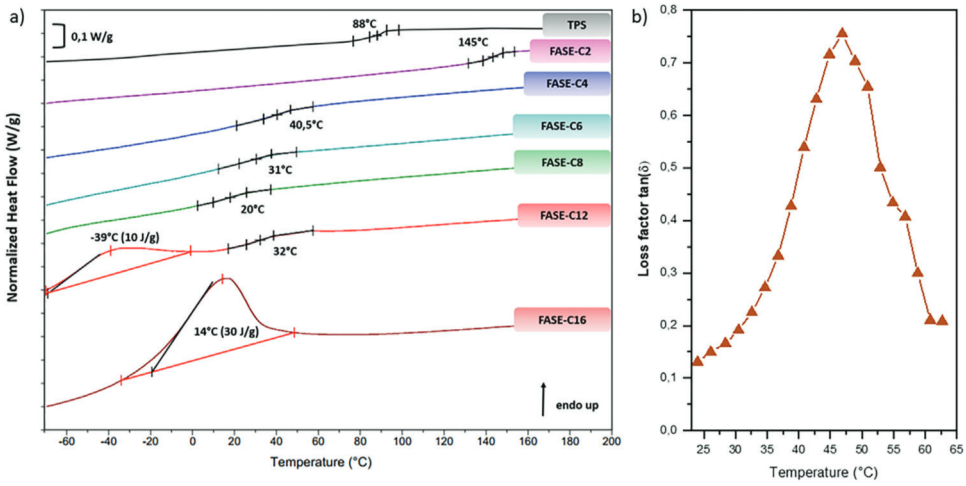

Figure 3. a) DSC thermograms of FASEs and TPS (second heating). b) Loss factor tan δ as a function of the temperature of FASE-C16.

cellulose esters.[23] Consequently, the diffraction peak at around $2\theta \approx 22°$ is rather a sign of an organization of the C16 part of the material.

At lower angles (2θ <10°), a peak (*) is observed whatever the FASE. This peak shifts to lower diffraction angles with the increase in the length of the alkyl chain. Vanmarcke et al. attribute this peak to the distance between starch chains which constitute the backbone of the macromolecule and propose a structural model where the starch backbones are organized in parallel planes separated by the alkyl chains, the latter being interpenetrated and/or tilted. This model has been formally proven for fatty chain lengths beyond C8.[20] The present study is in good agreement with these previous results for long alkyl chains and shows that this structural model remains valid for the shorter chain esters (from FASE-C2 to FASE-C8). In addition to the shift to lower diffraction angles, it appears that this peak became narrower and more intense when the side chain length increased indicating that an increase of this parameter favors the structural organization of the material.

2.2.2. Thermal Characterization

The thermograms recorded during the second heating (**Figure 3**a) reveal several thermal events: a glass transition characterized by a heat capacity jump and in some cases, an endotherm assigned to a melting.

Regarding the glass transition temperature (T_g) evolution as a function of the length of the alkyl chain, two kinds of behaviors can be observed. First, between the FASE-C2 and the FASE-C8, T_g decreases sharply as the length of the alkyl chain increases with a minimum of around 20 °C for FASE-C8. By comparison, TPS containing 12 wt% of water has a T_g ≈88 °C, that is, between that of the FASE-C2 and FASE-C4. This study reveals the efficiency of the internal plasticization of starch by alkyl chains from C2 to C8, the longer the alkyl chains are, the more they plasticize internally the material.

By contrast, between FASE-C8 and FASE-C12, an increase of T_g is observed with the alkyl chain length. This trend has already been noted for fatty acid cellulose esters,[23,28,29] as well as for starch fatty acid esters,[21] and it is explained by the fact that when the alkyl chains become longer (>C8), the very important steric hindrance thereof would hinder the movement of starch backbone chains and shift T_g to higher temperatures. In the case of FASE-C16, no T_g is clearly identified on the thermogram. To clarify this issue, DMA experiments were performed on this starch derivative from 20 to 65 °C, after heating the sample for 4 h at 70° in order to obtain FASE-C16 in a totally amorphous state, as we will show later in the paper. As illustrated in Figure 3b, the loss factor $\tan\delta = f(T)$ presents a maximum at around 47 °C corresponding to the main relaxation associated with the glass transition for FASE-C16.

Finally, thermal analyses reveal that both FASE-C12 and FASE-C16 exhibit an endotherm attributed to a melting process at around −39 and 14 °C with a low melting enthalpy of about 10 and 39 J g^{-1}, respectively. Note that for FASE-C12 and FASE-C16, the material exhibits a melting point below their glass transition. This particular behavior has already been observed for starch esters[20] and cellulose esters,[23,29] and also for other polymers having long side chains.[30,31] Based on the structural model described in the previous section, the origin of this behavior is explained by the fact that these two thermal events involve two different parts of the layered materials: the endotherm is linked to the melting of the part of the alkyl chains that has crystallized, whereas the glass transition concerns the main chain composed of the rigid skeleton of the starch.

2.2.3. Particular Thermal Behavior of FASE-C16

Unlike other starch esters with shorter chain lengths, the thermal behavior of FASE-C16 observed during the first and second heating is different as shown in **Figure 4**a.

Regarding the first heating (Figure 4a), two broad endotherms are observed: one of them is located toward 14 °C with a melting enthalpy of ≈4 J g^{-1} and a second one around 47 °C with a melting enthalpy of about 12 J g^{-1} attributed to the melting of thicker crystals or a more stable crystalline phase than the one

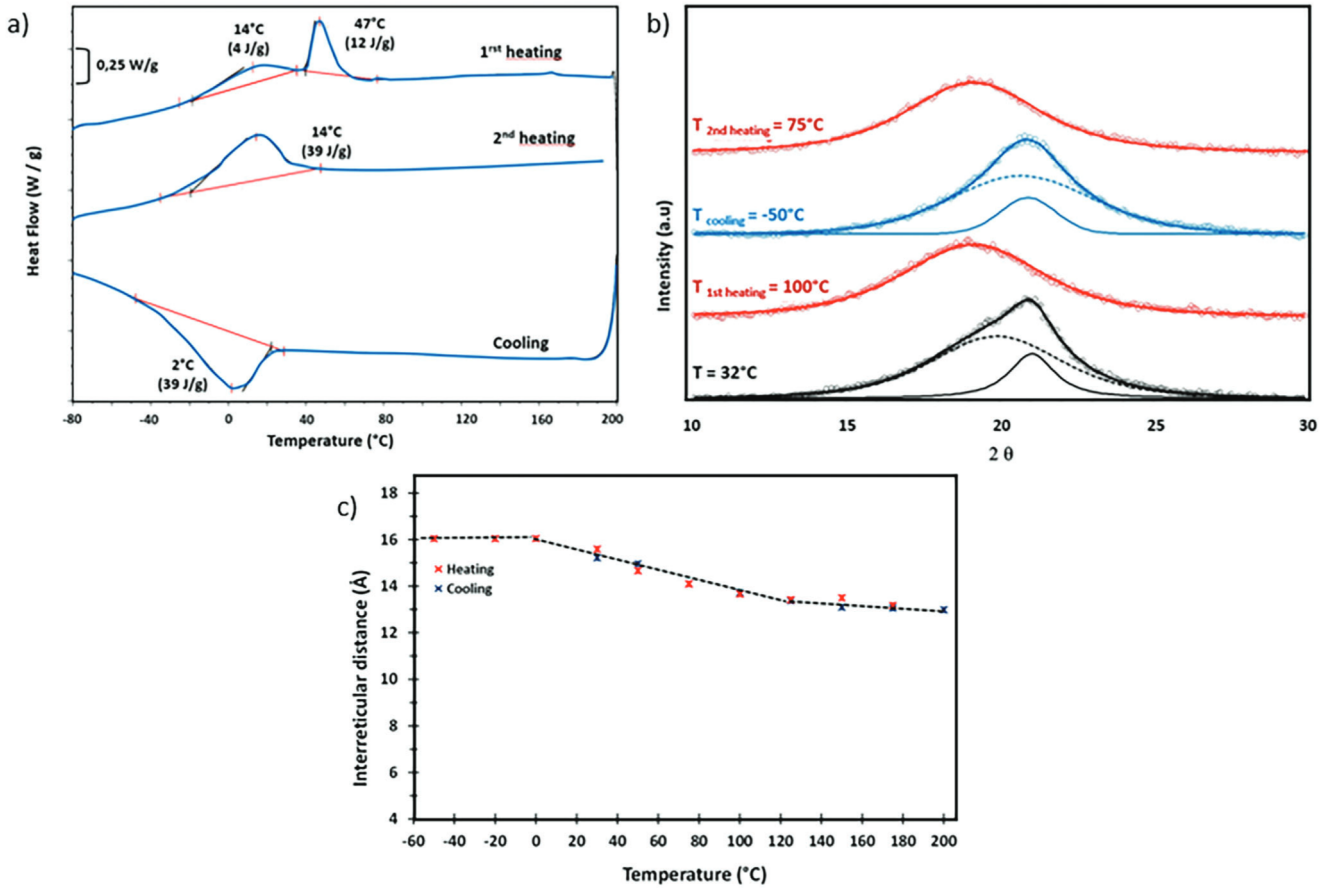

Figure 4. a) DSC thermograms of FASE-C16 recorded during the first heating, cooling, and second heating (endo up); b) WAXS profiles of FASE-C16 during first heating, cooling, and second heating; c) Interreticular distance of $2\theta = 2.8°$ as a function of temperature.

which melts at 14 °C. Note that these thicker or more stable crystals are responsible for the diffraction peak observed in Figure 2 for FASE-C16. During the second heating, only the endotherm at 14 ± 1 °C is observed with a much higher heat of fusion (≈39 J g^{-1}). Thick crystals or more stable crystals initially present in the sample seem to have recrystallized into smaller crystals, or in a less stable crystalline phase. Therefore, the initial sample is composed of two different populations of crystals or two crystalline phases of different stability. In response to this question, structural evolution as a function of temperature was studied by wide angle X-ray analyses from −50 to 200 °C upon heating and cooling at 10 K min^{-1} (Figure 4b) to compare with the results obtained by differential scanning calorimetry (DSC). During the first heating, between 32 and 100 °C, one can notice the disappearance of the crystalline peak at $2\theta \approx 22°$. This phenomenon may be ascribed to the crystal melting which takes place between 32 and 50 °C, according to the thermograms (Figure 4a). Regarding the amorphous halo, no significant evolution was observed except a small decrease in the position of the peak maximum related to the thermal expansion of the material occurring between 32 and 100 °C. Then, upon cooling, at −50 °C, the diffractogram recorded at −50 °C exhibits a crystalline peak at around $2\theta \approx 22°$. This result is in good agreement with the occurrence of the crystallization endotherm between 20 and −50 °C on the DSC thermogram showing that the crystalline phase formed on cooling has the same structure as the one in the initial sample. However, the crystalline peak in the diffractogram recorded at −50 °C is broader than the one for the initial sample. This suggests that the crystals formed on cooling are smaller leading to a lower melting point in the second heating. In particular, during the second heating, all crystals are melted at 40 °C.

For information, Figure 4c represents the evolution of the interreticular distance between planes containing the starch backbone. During heating, this interreticular distance decreases as the temperature is increased. This negative thermal expansion may be ascribed to a chain shortening of the alkyl chains due to torsional vibrations as it was previously reported in *n*-parafins.[32,33] Upon cooling, a reversible trend is observed, that is, an increase in the interreticular distance between planes containing the starch backbone.

2.3. Mechanical Behavior as Function of the Alkyl Chains Length

2.3.1. Mechanical Behavior of Starch Ester Films

The mechanical behavior upon uniaxial stretching of starch ester films was investigated. Note that it was not possible to test FASE-C2 which is extremely brittle. The engineering stress–strain curves are depicted in **Figure 5** for FASE-C4 to FASE-C16

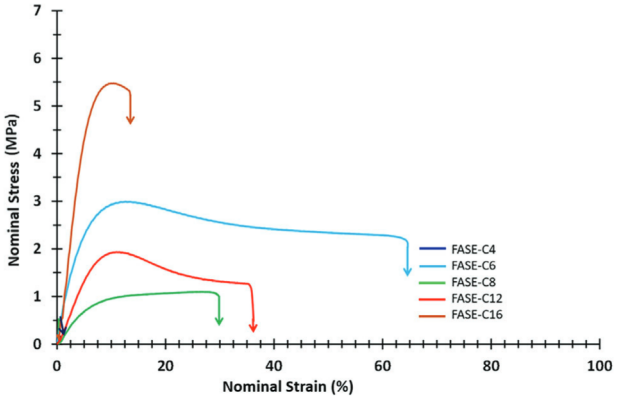

Figure 5. Stress–strain curves at 20 °C and 50% RH of acid starch ester at the strain rate 10^{-2} s^{-1}.

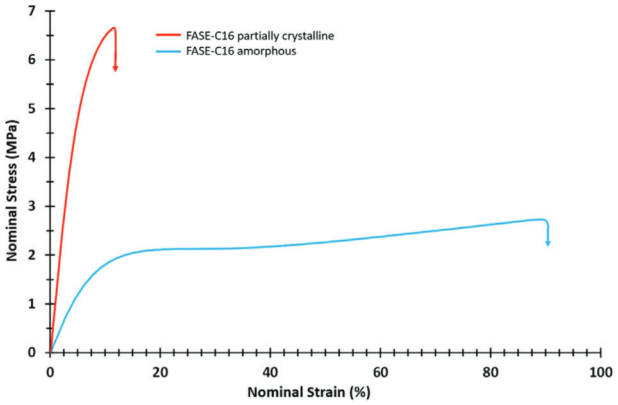

Figure 6. Stress–strain curves of FASE-C16 partially crystalline or totally amorphous (with and without crystals) under uniaxial tensile at 20 °C, 50% RH, and strain rate 10^{-2} s^{-1}.

Table 1. Mechanical properties of starch esters as a function of the alkyl chains length and TPS (determined at the strain rate of 10^{-2} s^{-1}).

Material	Young modulus E [MPa]	Tensile strength σ_b [MPa]	Strain at break [%]
TPS	1800 ± 114	39 ± 3	7 ± 3
FASE-C4	61 ± 16	0.5 ± 0.2	0.3 ± 0.1
FASE-C6	55 ± 12	3 ± 0.1	70 ± 32
FASE-C8	18 ± 10	1 ± 0.3	30 ± 16
FASE-C12	24 ± 5	1.6 ± 0.3	56 ± 25
FASE-C16	104 ± 3	6 ± 0.5	12 ± 2

and **Table 1** summarizes the Young modulus, tensile strength, and strain at break for starch esters and for pure TPS.

The mechanical behavior strongly depends on the alkyl chain length. While FASE-C4 is brittle, FASE-C6, FASE-C8, and FASE-C12 show a ductile behavior with a strain at break which can exceed 70%. The tensile strength is significantly lower than that of the TPS (σ_b = 39 ± 3 MPa) (Table 1). However, there is no clear evolution of the mechanical properties with the increase of alkyl chain length, in particular regarding Young's modulus and the strain at break. This ambiguous behavior could be rationalized by considering the thermal properties of the materials. For the FASE-C2 and FASE-C4, their glass transition temperature is higher than the drawing temperature (20 °C) which may explain their brittle behavior. For the FASE-C6, the T_g is close to room temperature. Consequently, the length of the alkyl chain seems sufficient to internally plasticize the material, as evidenced by the important deformation at the break achieved. A brittle/ductile transition seems to occur between FASE-C4 and FASE-C6. For ductile samples (FASE-C6, FASE-C8, FASE-C12), the evolution of the Young modulus and tensile strength follows the same trend as T_g: FASE-C8 which has the lowest T_g and exhibits the weakest E and σ_b. FASE-C12 shows a slight increase in these two parameters in comparison with FASE-C8. As already mentioned for T_g, this phenomenon could be related to the steric hindrance of the alkyl chains which would hinder the mobility of the starch backbone from which the results obtained.

2.3.2. Mechanical Behavior of FASE-C16

Within the literature, the properties of FASE-C16 with a DS close to 3 are extremely variable from one study to another. In some cases, the material appears rather ductile,[22] while in other cases it is brittle.[20,21] This could be due to the methods of synthesis and elaboration which are sometimes very different from one study to another. But currently, to our knowledge, no explanation has been proposed in the literature. In the present study, as shown in Figure 5 and Table 1, a decrease of the strain at the break with a significantly higher young modulus and stress level was observed for FASE-C16, in comparison with other FASEs. This result could be explained by the fact that, unlike other chain lengths, FASE-C16 is, as previously discussed, semi-crystalline at room temperature (Figure 4, first heating). In addition, as determined by DMA analysis, it is highly likely that the glass transition temperature (related to the starch chains) of FASE-C16 is around 47 °C, that is, higher than that measured for FASE-C12 ($T_g \approx 32$ °C). These two phenomena could consequently increase the rigidity of the material, hence the increase in the stress level. Another explanation for the low strain at break could be that for the FASE-C16 of DS ≈ 3, 16 carbons length fatty chain would inhibit the entanglements of the starch chains because of its steric hindrance. In order to confirm one of these two assumptions (crystals or entanglements), tensile tests were carried out on samples having undergone a thermal treatment for 4 h at 70 °C in order to remove the crystals within the material as was previously shown in the thermal study and then drawn at room temperature. The results are shown in **Figure 6**.

It appears that the disappearance of the crystals within the material leads to a ductile behavior with a strain at a break of 90 ± 20%, a Young modulus of 30 ± 10 MPa, and a stress level of 2.7 ± 0.2 MPa against 12 ± 2%, 104 ± 3 Mpa, and 6 ± 0.5 MPa for the initial sample, respectively. According to the thermogram of Figure 4a, beyond 70 °C, the crystals have completely melted and are reformed during cooling at a temperature below room temperature ($T \approx 4$ °C). Annealing FASE-C16 for 4 h at 70 °C followed by cooling at room temperature thus eliminated the crystals initially present in the material, explaining the lower Young modulus and stress level by comparison with the initial sample. Also,

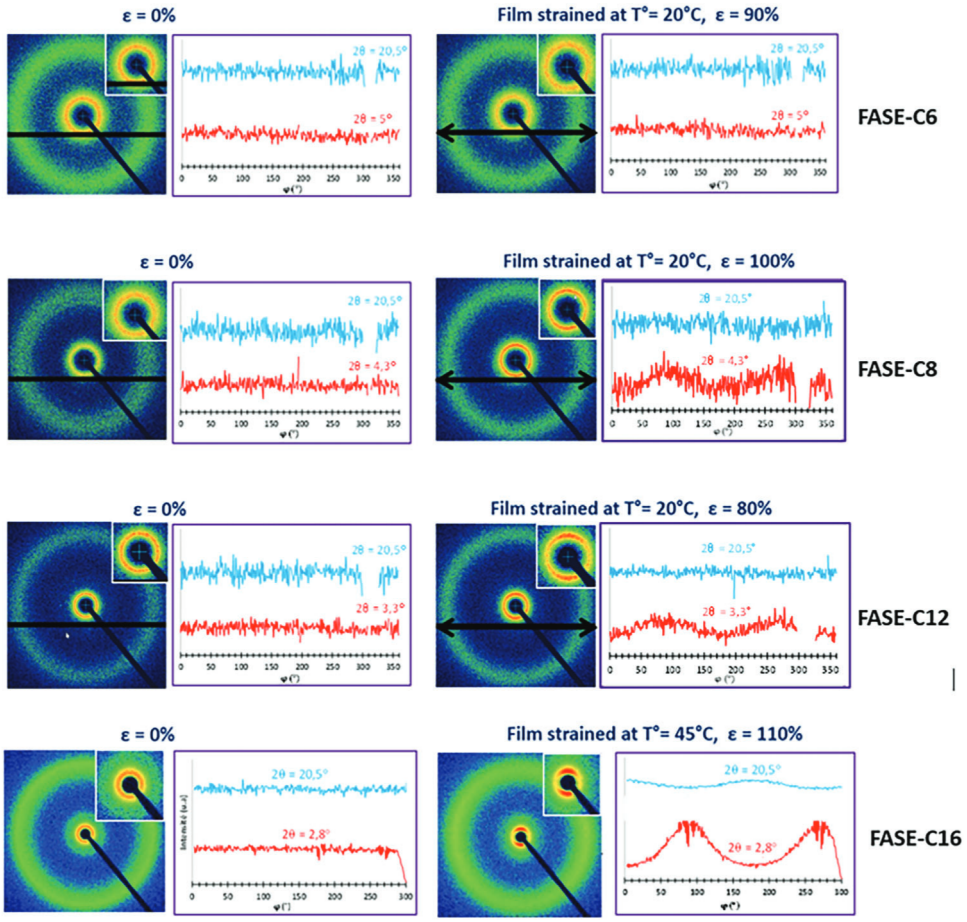

Figure 7. Strain-induced structural evolution of starch ester samples (from C6 to C16) using X-ray diffraction analyses. Post-Mortem WAXS patterns of samples uniaxially stretched (horizontal draw direction).

we can conclude that the initial sample of FASE-C16 was brittle because of the presence of the crystals. Note that a slight strain hardening phenomenon can be observed in the plastic regime for the FASE-C16 without crystals. This phenomenon can result from the strain-induced chain orientation, as shown in the next session of the paper.

As in this study, Vanmarcke et al.,[20] as well as Winkler et al.,[21] also observed a brittle behavior of FASE-C16 (with DS ≈ 3) at room temperature and both highlighted the presence of a melting endotherm above room temperature. By contrast, Yan et al.,[22] report a rather ductile behavior for the FASE-C16 (with DS ≈ 3) and only mention the presence of a glass transition temperature. In view of all of these results, it can be concluded that the presence or not of crystals in the sample can explain the different mechanical behaviors reported in the literature.

It should be mentioned that the presence or absence of crystals is not due to the synthesis methods but rather to the aging of the sample. The DSC curve recorded during the cooling step at −10 °C min^{-1} shows a crystallization exotherm just below room temperature (Figure 4a). Therefore, the film stored at room temperature will be gradually able to crystallize over time. This phenomenon, which corresponds to annealing at room temperature or aging, explains the origin of the melting peak at about 47 °C, observed during the first heating of FASE-C16: the crystals formed at room temperature during the storage time of the film (between the time of elaboration and analysis) will melt just above the "annealing/aging temperature." It is therefore expected that the mechanical behavior of FASE-C16 will change with storage time. In particular, the stress level will increase at the expense of the elongation at break with aging.

2.4. Macromolecular Orientation during Uniaxial Stretching Test as Function of the Length of Alkyl Chain

In order to gain a better understanding of the structure-property relationships upon stretching, the strain-induced structural evolution of FASE-C6 to FASE-C16 samples has been studied using X-ray diffraction analyses. **Figure 7** displays the post-mortem X-ray patterns of stretched samples. In order to prevent as much as possible macromolecular relaxation, samples were cooled to −55 °C before unloading.

Before stretching, all samples are isotropic. For the FASE-C6 sample, no indication of macromolecular orientation is observed after stretching as revealed by the well-defined diffraction rings located at $2\theta = 5°$ and 20°. Two hypotheses can explain this result: either a relaxation of the starch backbone chains takes place dur-

ing drawing, or it takes place between sample unloading and the X-ray diffraction analysis despite the experimental precautions.

In the case of FASE-C8 and FASE-C12, the diffraction patterns associated with the deformed samples show that the intensity of the most intense ring is heterogeneous suggesting a macromolecular orientation. The azimuthal integration of the most intense reflection ($2\theta = 4.3°$ and 3.3°, respectively) assigned to the planes containing the starch chains reveals that starch chains tend to orient toward the stretching direction. Surprisingly, no orientation of the amorphous phase is observed (reflexion at $2\theta = 20.5°$). Note that the orientation of starch chains seems less pronounced than in a previous study.[20] This difference could be due on one hand, to the fact that contrary to the study of Vanmarcke et al., we are dealing in the present case with a post-mortem study and some chain relaxation can occur and on the other hand, to the difference in the botanical origin of starch used for the preparation of the samples.

Unlike the previous samples stretched at room temperature, FASE-C16 was deformed at 45 °C, in order to deform it. Pattern analysis, as well as azimuthal integrations of the two main reflections ($2\theta = 2.8°$ and 20.5°), clearly show a macromolecular orientation in the sample. The intensity of the reflection located at $2\theta = 2.8°$ is much more pronounced at the equator, confirming that starch backbones are oriented toward the draw direction. Regarding the reflection at $2\theta = 20.5°$, the azimuthal integration suggests a maximum intensity in the draw direction. This could be attributed to the reflection of the alkyl chains which are perpendicular to the starch chains according to the structural model proposed for long-chain FASEs.[20]

3. Conclusion

Structural, thermal, and mechanical properties of fully substituted acid starch esters have been investigated in relation to side chain length varying from C2 to C16. This study reveals that the substitution of hydroxyl function by alkyl chains is an interesting way to plasticize starch. FASE with C2 to C12 side chains are fully amorphous with a glass transition temperature depending on chain length while a fraction of C16 side chains is able to crystallize at a temperature close to ambient conditions. The mechanical behavior depends on the side chain length. In particular, this study shows that the side chain length should contain between 6 to 12 carbons to have a ductile behavior. Several applications may be considered for these ductile FASEs such as in packaging. Future work will focus on in situ X-ray diffraction experiments during stretching to better understand the origin of the stretchability enhancement of starch esters and on measurements of gas barrier properties (oxygen...) to evaluate their potential application in food packaging.

4. Experimental Section

Materials: Waxy maize starch was selected for the synthesis of the starch esters because it is composed of 100% amylopectin chains. Native starch granules were supplied by Roquette Frères (Lestrem, France). Prior to chemical modification, starch granules were oven-dried at 105 °C for 24 h and stored in a desiccator. Waxy maize starch acetate was synthesized and supplied by Roquette Frères (Lestrem, France) and is a commercial product. All reagents were stored at room temperature and used without further purification: pyridine (99%, Aldrich); butyryl chloride (BCl, 98% Aldrich); hexanoyl chloride (HCl, 99% Aldrich); octanoyl chloride (OCl, 99%, Aldrich); lauroyl chloride (LCl, 98%, Aldrich); palmitoyl chloride (PCl, 98%, Acros); chloroform (≥99%, Carlo Erba); ethanol (≥99%, Carlo Erba). Deuterated chloroform used for NMR analyses was purchased from Sigma Aldrich and stored at 4 °C.

Synthesis of Acylation of Starch by Acyl Chlorides: Acylation of starch samples with chain acids was performed using a procedure adapted from literature.[19] In a typical experiment, 20 g of dried starch was dissolved in 200 mL of pyridine at 90 °C for 30 min until complete solubilization of starch. 200 mL of acyl chloride was then added, whatever the length of the alkyl chains, and the mixture was stirred and classically heated at 90 °C for 3 h. The product was then poured into ethanol (1.2 L for octanoate, laurate, and palmitate fatty starch esters) or an ethanol/water mixture (10/1 for hexanoate and 2/1 for butyrate starch ester) to precipitate acid starch ester and the solid was recovered by filtration and purified by a repeated solubilization/precipitation process using chloroform and ethanol or ethanol/water mixture, respectively, depending of materials as described previously. The products, which were then dried in air at room temperature for 2 weeks, look like light-yellow powders (solid).

In order to obtain a reference material, the same chemical treatment was applied to the starch without the addition of acid chlorides in order to be able to determine whether the synthesis conditions generated changes in the starch. This material is referenced as TPS in this study.

Substituted FASE samples with different length chains will be named in this paper FASE-C*x*, with *x* corresponding to the number of carbon on the alkyl chain.

Chemical Characterization: Every product was characterized by Fourier-transformed infrared (FTIR) spectroscopy using a Perkin-Elmer Spectrum 100 apparatus equipped with an ATR accessory, to probe the efficiency of reactions. Each Spectrum was normalized using the 1050 cm^{-1} band corresponding to the vibration of the C—O—C bonds of the starch glucosic units.

^1H NMR spectra were performed in $CDCl_3$ using a Bruker DRX-300 Spectrometer (operating at 300 MHz) to assess purity and determine the DS of FASEs by an integration method described in ref.[34].

Samples Elaboration and Storage Conditions: Every product was converted into 200 µm thick film by compression molding ($P = 10$ bars, $t = 5$ min) with a temperature ranging from 120 to 200 °C according to sample chemical composition, that is, 200 °C for FASE-C2, 130 °C for FASE-C4, and 120 °C for FASE-C6, FASE-C8, FASE-C12, and FASE-C16. The molding temperature optimized through preliminary tests was generally around T_g + 70 °C, that is, well below the degradation temperature of all products (see TGA curves in Supporting Information). In the case of TPS, according to literature,[35] starch was hydrated until reaching a global water content of 30% wet basis, the day before compression molding. Then, compression molding of TPS films was performed at 130 °C.

Prior to any characterization, all films were stored under ambient conditions (20 °C, 57% relative humidity [RH]) for 1 week in order to reach the moisture content equilibrium notably for TPS. In the case of TPS, this ensured to work at a constant water content of 12 wt%. In the case of starch esters, as expected, the chemical modification limited its water uptake which was lower than 0.5 wt% for all products.

Structural Characterization: WAXS analysis was carried out at room temperature in transmission mode on starch ester films. The analyses were performed on a Xeuss apparatus (Xenocs, France) and the Cu-Kα radiation ($\lambda = 1.54$ Å) was used. The sample-to-detector distance, around 12 cm, was calibrated using Silver Behenate as a calibrant. The WAXS patterns were recorded on a Pilatus detector (Dectris). The intensity profiles were obtained by 360° azimuthal integration and from 1° to 35° radial integration of the 2D patterns using the Foxtrot software. For some tests, initial samples were heated using a heating stage (Linkam HFSX350) in the temperature range of −90 to 200 °C at heating and cooling rates of 10 °C min^{-1} during the WAXS experiments.

Thermal Characterization: DSC experiments were carried out on a DSC Q2000 (Thermal Analysis) instrument calibrated with a high-purity indium sample according to standard procedures. The samples of ≈15 mg were put in sealed pans and analyzed in the temperature range from −80 to

200 °C at a heating/cooling rate of ±10 °C min^{-1} under a nitrogen atmosphere. Thermal properties were measured during the second heating, the glass transition temperature T_g was measured halfway up the heat capacity jump, and the melting temperature T_m was taken at the maximum of the melting peak.

Dynamic mechanical analysis (DMA) experiments were performed on a Rheometrics RSA III apparatus operating in tensile mode at a frequency of 1 Hz in the temperature range of 25 < T < 60 °C. Specimen gauge width and length of 5 mm × 15 mm were cut out from the films. The main relaxation temperature associated with the glass transition was taken to the peak maximum of the loss factor tan δ.

Uniaxial Tensile Behavior: Mechanical behavior was studied in uniaxial tensile mode using an Instron 4466 apparatus. Experiments were performed at an initial strain rate of 10^{-2} s^{-1} at room temperature under 50% RH. Dumbbell-shaped specimens with gauge width and length of 5 mm × 24 mm, respectively, were laser cut out from the starch ester films.

Supporting Information

Supporting Information is available from the Wiley Online Library or from the author.

Acknowledgements

IFMAS (Institut Français des Matériaux Agro-Sourcés) and ANR are gratefully acknowledged for their financial support. This project was supported by the French government as part of the "Programme d'Investissement d'Avenir." The project ARCHI-CM, Chevreul Institute (FR 2638), Ministère de l'Enseignement Supérieur et de la Recherche, Région Hauts-de-France, and European Regional Development Fund (FEDER) are acknowledged for supporting and funding this work.

Conflict of Interest

The authors declare no conflict of interest.

Data Availability Statement

The data that support the findings of this study are available from the corresponding author upon reasonable request.

Keywords

biopolymers, mechanical properties, starch ester, structural evolution

Received: June 6, 2023
Revised: July 21, 2023
Published online:

[1] L. Avérous, *J. Macromol. Sci., Polym. Rev.* **2007**, *44*, 231.
[2] A. Jiménez, M. J. Fabra, P. Talens, A. Chiralt, *Food Bioprocess Technol.* **2012**, *5*, 2058.
[3] T. Mekonnen, P. Mussone, H. Khalil, D. Bressler, *J. Mater. Chem. A* **2013**, *1*, 13379.
[4] P. J. Halley, L. Avérous, *Starch Polymers: From Genetic Engineering to Green Applications*, Elsevier, Amsterdam **2014**.
[5] Q. Chen, H. Yu, L. Wang, Z. Abdin, Y. Chen, J. Wang, W. Zhou, R. Yang, R. Khan, H. Zhang, X. Chen, *RSC Adv.* **2015**, *5*, 67459.
[6] T. N. Prabhu, K. Prashantha, *Polym. Compos.* **2018**, *39*, 2499.
[7] C. E. Montilla-Buitrago, R. A. Gómez-López, J. F. Solanilla-Duque, L. Serna-Cock, H. S. Villada-Castillo, *Starch* **2021**, *73*, 2100060.
[8] L. Avérous, P. J. Halley, *Biofuels, Bioprod. Biorefin.* **2009**, *3*, 329.
[9] S. H. D. Hulleman, F. H. P. Janssen, H. Feil, *Polymer* **1998**, *39*, 2043.
[10] F. J. Rodriguez-Gonzalez, B. A. Ramsay, B. D. Favis, *Carbohydr. Polym.* **2004**, *58*, 139.
[11] D. Lourdin, L. Coignard, H. Bizot, P. Colonna, *Polymer* **1997**, *38*, 5401.
[12] X. Ma, J. Yu, J. Feng, *Polym. Int.* **2004**, *53*, 1780.
[13] A. Sankri, A. Arhaliass, I. Dez, A. C. Gaumont, Y. Grohens, D. Lourdin, I. Pillin, A. Rolland-Sabaté, E. Leroy, *Carbohydr. Polym.* **2010**, *82*, 256.
[14] H. Schmitt, A. Guidez, K. Prashantha, J. Soulestin, M. F. Lacrampe, P. Krawczak, *Carbohydr. Polym.* **2010**, *115*, 364.
[15] L. Zhang, W. Xie, X.i Zhao, Y. Liu, W. Gao, *Thermochim. Acta* **2009**, *495*, 57.
[16] A. David, J. Meimoun, T. Delaunay, V. Wiatz, R. Saint-Loup, J. Parcq, N. Descamps, A. Favrelle, F. Bonnet, G. Stoclet, D. Lourdin, P. Zinck, V. Gaucher, *eXPRESS Polym. Lett.* **2019**, *13*, 235.
[17] S. E. Barrios, G. Giammanco, J. M. Contreras, E. Laredo, F. López-Carrasquero, *Int. J. Biol. Macromol.* **2013**, *59*, 384.
[18] T. Liebert, M. C. V. Nagel, T. Jordan, A. Heft, B. Grünler, T. Heinze, *Macromol. Rapid Commun.* **2011**, *32*, 1312.
[19] H. Winkler, W. Vorwerg, H. Wetzel, *Carbohydr. Polym.* **2013**, *98*, 208.
[20] A. Vanmarcke, L. Leroy, G. Stoclet, L. Duchatel-Crépy, J.-M. Lefebvre, N. Joly, V. Gaucher, *Carbohydr. Polym.* **2017**, *164*, 249.
[21] H. Winkler, W. Vorwerg, R. Rihm, *Carbohydr. Polym.* **2014**, *102*, 941.
[22] B. Y. Yang, R. Montgomery, *Starch - Stärke* **2008**, *60*, 146.
[23] L. Crépy, V. Miri, N. Joly, P. Martin, J.-M. Lefebvre, *Carbohydr. Polym.* **2011**, *83*, 1812.
[24] J. Aburto, I. Alric, S. Thiebaud, E. Borredon, D. Bikiaris, J. Prinos, C. Panayiotou, *J. Appl. Polym. Sci.* **1999**, *74*, 1440.
[25] N. W. H. Cheetham, L. Tao, *Carbohydr. Polym.* **1998**, *36*, 277.
[26] H. F. Zobel, *Starch - Stärke* **1988**, *40*, 44.
[27] A. Imberty, S. Perez, *Biopolymers* **1988**, *27*, 1205.
[28] T. Morooka, M. Norimoto, T. Yamada, N. Shiraishi, *J. Appl. Polym. Sci.* **1984**, *29*, 3981.
[29] J. E. Sealey, G. Samaranayake, J. G. Todd, W. G. Glasser, *J. Polym. Sci., Part B: Polym. Phys.* **1996**, *34*, 1613.
[30] E. F. Jordan, D. W. Feldeisen, A. N. Wrigley, *J. Polym. Sci., Part A: Polym Chem* **1971**, *9*, 1835.
[31] F. Lopez-Carrasquero, A. Martinez de Ilarduya, M. Cardenas, M. Carillo, M. L. Arnal, E. Laredo, C. Torres, B. Méndez, A. J. Müller, *Polymer* **2003**, *44*, 4969.
[32] G. T. Davis, R. K. Eby, J. P. Colson, *J. Appl. Phys.* **1970**, *41*, 4316.
[33] N. O. B. Lüttschwager, M. A. Suhm, *Soft Matter* **2014**, *10*, 4885.
[34] N. Joly, R. Granet, P. Branland, B. Verneuil, P. Krausz, *J. Appl. Polym. Sci.* **2005**, *97*, 1266.
[35] G. Coativy, N. Gautier, B. Pontoire, A. Buléon, D. Lourdin, E. Leroy, *Carbohydr. Polym.* **2015**, *116*, 307.